Cellular Signaling

DOI: 10.1002/anie.201001149

Artificial Control of Cell Signaling and Growth by Magnetic Nanoparticles**

Jae-Hyun Lee, Eun Sook Kim, Mi Hyeon Cho, Mina Son, Soo-In Yeon, Jeon-Soo Shin, and Jinwoo Cheon**

In memory of Chi Sun Hahn

Mechanical stresses on biological objects can lead to changes in a wide range of cellular properties, such as cell shape, cytoskeletal organization, and cell fate, by means of physical stimulations using dielectricity, optical trapping, and magnetic cytometry.[1–8] In particular, micrometer-sized magnetic beads have been useful since their first utilization by Crick and Hughes to draw mechanical stresses on biological objects by developing techniques such as magnetic twisting, pulling, and cell-stretching cytometry.[5–8] With the use of such magnetic stimulations, the roles of mechanical stresses for cell characteristics have been studied, which include cytoplasmic viscosity, cytoskeletal mechanotransduction, and mechanical calcium responses.[5–10]

Further scientific breakthroughs in this research field have depended on molecular-level understanding of mechanobiological processes and the induction of changes in cellular functions and/or cytoskeletal structures. The goal is to bring about single-cell or subcellular-level imaging and actuation of biological objects with high target specificity. Nanoscale probes and actuators are important because of their small sizes, which are comparable to those of many biologically meaningful molecules such as DNAs and proteins. In addition, their ability to attach multivalence functional groups would be another advantage. By employing nanoparticles, difficult challenges associated with currently used micrometer-scale magnetic particles, such as probing and manipulation of a single receptor without disturbing any other rheological or cytoskeletal properties of the entire cell, can be overcome.

Recently, the groups of Ingber and Dobson have independently demonstrated that activation of ion channels is possible by using nanoscale magnetic particles.[11–13] These efforts have demonstrated that FcεRI, a cellular membrane receptor, can be magnetically agglomerated to activate the Ca^{2+} signal.[11] On the other hand, TREK-1, a membrane protein for the K^+ ion channel, is specifically activated by magnetic nanoparticles with size as small as 130 nm.[13] While these two pioneering works focused on ion-channel activations, new conceptual advances and other applications of nanoscale magneto-activated cellular signaling (N-MACS) are widely open to exploration.

Herein, we demonstrate for the first time that receptor-mediated artificial triggering of cell growth in the preangiogenesis stage is possible by the N-MACS approach. Angiogenesis is a vital process both for the growth and development of blood vessels and for tumor metastasis.[14] Conventionally, this process is initiated by several interactions that take place between specific receptors and ligands on the cell surface.[15,16] The Tie2/angiopoietin (Ang) pair, in which one Ang molecule binds to clusterize three to five Tie2 receptors, is regarded as one of the important receptor–ligand interactions.[17–19] This cluster formation is critical to activate multiple signaling steps and eventually participates in the angiogenic processes.[18–20]

Instead of using such ligands, in our study a TiMo214 monoclonal antibody (mAb)-conjugated Zn^{2+}-doped ferrite magnetic nanoparticle (Ab-Zn-MNP) is employed to target and magnetically manipulate Tie2 receptors through the steps in Figure 1 a–c. To achieve this result, two permanent NdFeB magnets are positioned to exert an external magnetic field of about 0.15 T, with horizontal magnetic field lines that are oriented in the manner shown in Figure 1 d. At this magnetic field strength, magnetization of Ab-Zn-MNPs can be saturated in plane (Figure 1 e), which induces strong attractive forces between the dipoles of neighboring nanoparticles. This phenomenon results in the aggregation of Ab-Zn-MNPs.

For successful magnetic manipulation under mild external magnetic field conditions, we utilized a high-performance 15 nm Zn^{2+}-doped ferrite magnetic nanoparticle (Zn-MNP) instead of a conventional magnetic nanoparticle, since it exhibits a very high saturation magnetization (Figure 1 e,f)

[*] J.-H. Lee,[+] M. H. Cho, Prof. J. Cheon
Department of Chemistry, Yonsei University
Seoul 120-749 (Korea)
Fax: (+82) 2-364-7050
E-mail: jcheon@yonsei.ac.kr
E. S. Kim,[+] M. Son, S.-I. Yeon, Prof. J.-S. Shin
Department of Microbiology
Institute for Immunology and Immunological Diseases
College of Medicine, Yonsei University
Seoul 120-752 (Korea)
Fax: (+82) 2-392-7088
E-mail: jsshin6203@yuhs.ac
[+] These authors contributed equally to this work.

[**] We thank Prof. Gou Young Koh (KAIST) for recombinant Ang2 and his kind support. This research was supported by the NRL (M10600000255), Creative Research Institute (2010-0018286), WCU program, NBIT (Grant K20716000001-07A0400-00110), Nanomedical NCRC (R15-2004-024-00000-0), LG Yonam Foundation, 2nd stage BK21 for Chemistry and Medical Sciences of Yonsei University, the Korean Health 21 R&D Project (A050260) of the Ministry of Health & Welfare, the KRF Grant (KRF-2007-2-E00154), and Mid-career Researcher Program (2009-0081001) through NRF by the MEST.

Supporting information for this article is available on the WWW under http://dx.doi.org/10.1002/anie.201001149.

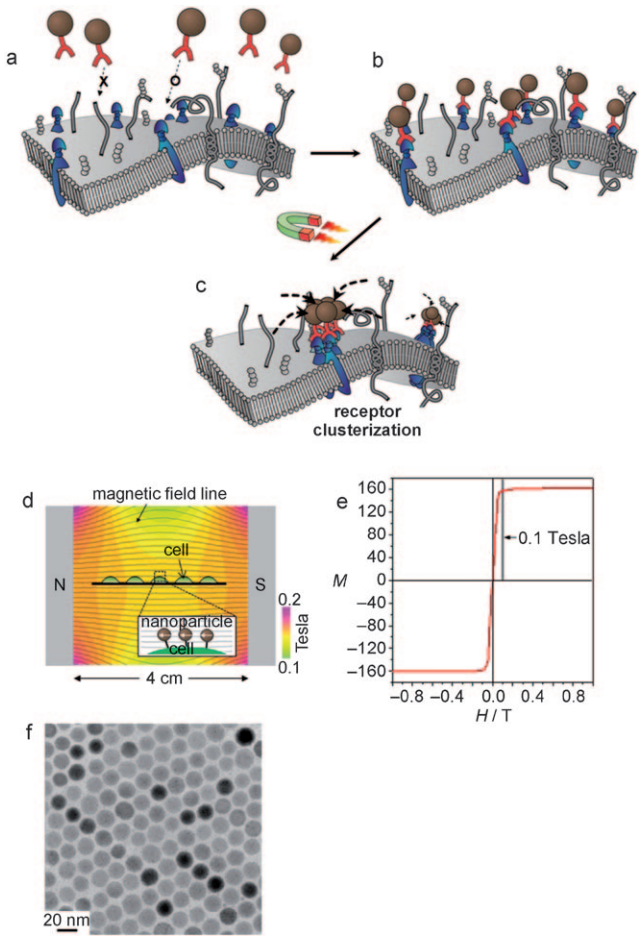

Figure 1. a–c) Targeting and magnetic manipulation of Ab-Zn-MNPs. a,b) Ab-Zn-MNPs selectively bind to the specific cell-surface Tie2 receptors. c) In the presence of an external magnetic field, the Ab-Zn-MNPs are magnetized to form nanoparticle aggregates, which then induce the clustering of receptors to trigger intracellular signaling. d) Magnet setup and the simulated magnetic field. The inset shows magnetized nanoparticles on the cell surface. e) *M*–*H* curve of Zn-MNPs measured by using a superconducting quantum interference device (SQUID); *M* in emu per g magnetic atom. Zn-MNPs have a strong saturation magnetization value (ca. 160 emu per g magnetic atom) and high magnetic susceptibility ($\chi_m = 6.53 \times 10^{-2}$) which saturates at low magnetic fields below 0.1 T. f) Transmission electron microscopy (TEM) image of Zn-MNPs.

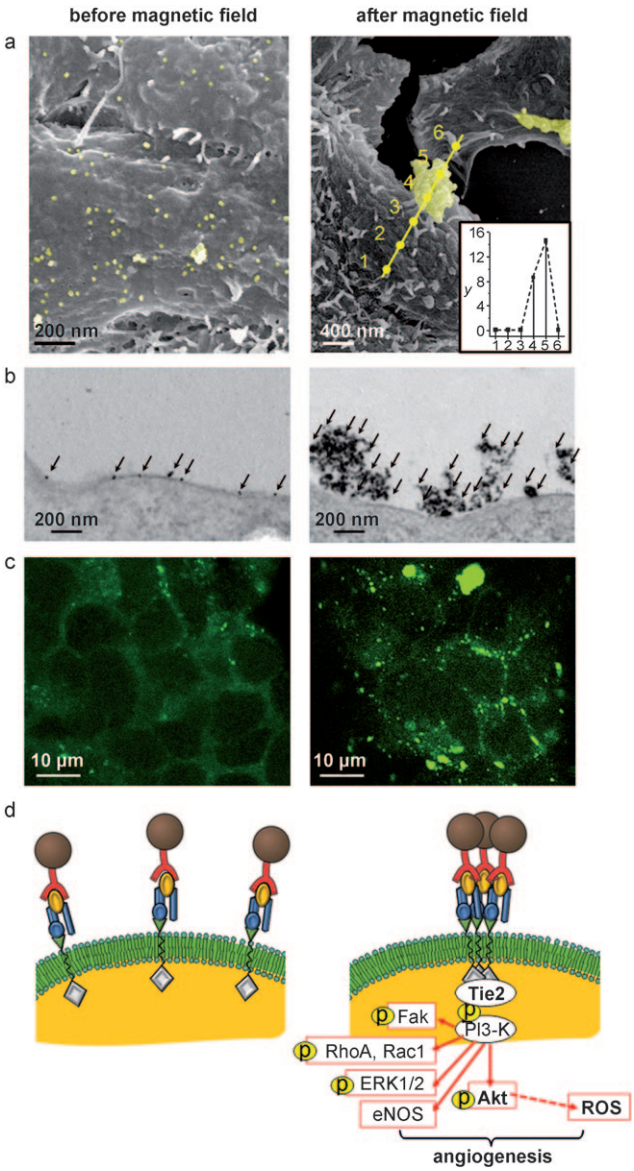

Figure 2. Magnetism-induced aggregation of Ab-Zn-MNPs on the 293-hTie2 cell surface. a) SEM images of the nanoparticles. The inset in the image on the right shows EDX spot analysis on the aggregate, which indicates a high Fe content (*y* in atom %) of Ab-Zn-MNPs. Nanoparticles in the SEM images are false-colored as yellow for clear visibility. b) TEM images of the nanoparticles. Nanoparticles are indicated by arrows. c) Fluorescence confocal microscopy images of nanoparticles before and after application of a magnetic field. d) Tie2 receptor-bound nanoparticles before and after application of the magnetic field.

superior to that of conventional nanoparticles, such as Feridex (ca. 80 emu per g magnetic atom).[21] Also, Zn-MNP has a strong magnetic susceptibility that enables fast saturation of magnetization under a magnetic field strength of about 0.1 T (Figure 1 e). The magnitude of its tensional force is calculated to be around 10^{-17} N, which is adequate to induce only receptor clusterization, but small enough not to alter the cell shape or cytoskeletal organization.[10,11]

The Ab-Zn-MNP conjugate (4 µg) was used to treat 4×10^6 293-hTie2 cells,[22] modified to overexpress Tie2 from the HEK293 cell line, in a petri dish at room temperature. After 30 min, unbound nanoparticles were removed by washing and the dish was placed in a magnetic field (ca. 0.15 T) for 1 h. Most of the nanoparticles were on the cell surface at this stage. The evenly dispersed Ab-Zn-MNPs on the cell surface aggregated after application of the magnetic field, as seen by scanning electron microscopy (SEM) and TEM (Figure 2 a,b). Energy-dispersive X-ray (EDX) spot analysis of the aggregates showed that there was a high content of atomic Fe, thus confirming that the aggregates are indeed magnetic nanoparticles (Figure 2 a, inset).

Ab-Zn-MNP was also used as a fluorescence imaging probe after labeling with fluorescein. Application of the magnetic field to cells containing Ab-Zn-MNP/fluorescein resulted in a change of fluorescence distribution on the cell surface, from a weak and evenly dispersed green fluorescence to several bright, strongly fluorescent clumps (Figure 2c), which suggests that clustering of both Ab-Zn-MNPs and Tie2 receptors occurs. Clustering of Tie2 receptors can induce intracellular signaling processes that lead to angiogenesis. This takes place through several downstream signaling gateways, including phosphorylation of Tie2 and further propagation to phosphorylation of Akt, Fak, RhoA, Rac1, and ERK1/2, and the formation of endothelial nitric oxide synthase (eNOS) and reactive oxygen species (ROS) (Figure 2d, right picture).[18,20]

The formation of phosphorylated Tie2 (p-Tie2), which is the first gateway for signaling, is promoted only when cells are treated with Ab-Zn-MNPs followed by application of a magnetic field (Figure 3a–c). Western blots (Figure 3b) show that a strong band for p-Tie2 is present only in lanes 5, 7, and 9 (boxed), which corresponds to the cells that are first treated with Ab-Zn-MNPs and then subjected to a magnetic field. In contrast, other cells, which are treated with Zn-MNP (lane 2), Ab (lane 3), and Ab-Zn-MNP but are not subjected to a magnetic field (lanes 4, 6, and 8), exhibit negligibly weak bands for p-Tie2. In the presence of a magnetic field, the relative expression of p-Tie2 is dependent on the amount of Ab-Zn-MNP used to treat the cells, and increases from 3.3 to 4.1 and 4.5 as the amount of Ab-Zn-MNP increases from 2 to 4 and 8 μg. In contrast, the expression of p-Tie2 remains almost constant when a magnetic field is not applied (Figure 3c; also see lanes 4, 6, and 8 of Figure 3b). Here, the ratio of Ab to Zn-MNP is strictly controlled as 1:1, to avoid multiple binding of one nanoparticle to several receptors (see the Supporting Information, Figure S4).

Magnetic-field-induced downstream signaling associated with phosphorylation of Akt (p-Akt) is confirmed by using fluorescence confocal microscopy on immunofluorescent-stained cells (Figure 3d–f). In this procedure, Ab-Zn-MNP labeled with green-fluorescent fluorescein is used. In addition, the resulting p-Akt is labeled to emit red fluorescence by using anti-p-Akt immunoglobulin G (IgG) and its secondary antibody, Alexa 594-labeled anti-rabbit IgG. Upon application of a magnetic field, Ab-Zn-MNPs aggregate and appear as bright green fluorescing clumps (Figure 3e, 1) and the red fluorescence indicates the phosphorylation of Akt (Figure 3e, 2). The areas of green fluorescence overlaps nicely with areas exhibiting p-Akt red fluorescence, where the overlapped regions appear yellow (Figure 3e, 3). This result indicates that p-Akt is abundant in the regions where Ab-Zn-MNP aggregates are present. In contrast, when a magnetic field is not applied, the aggregation of Ab-Zn-MNPs or p-Akt is not observed (Figure 3f). In addition, the formation of ROS, another signaling product, is also observed by using fluorescence confocal microscopy only when the external magnetic field is applied (Supporting Information, Figure S5). The combined results provide strong evidence that aggregation of magnetic nanoparticles takes place when an external mag-

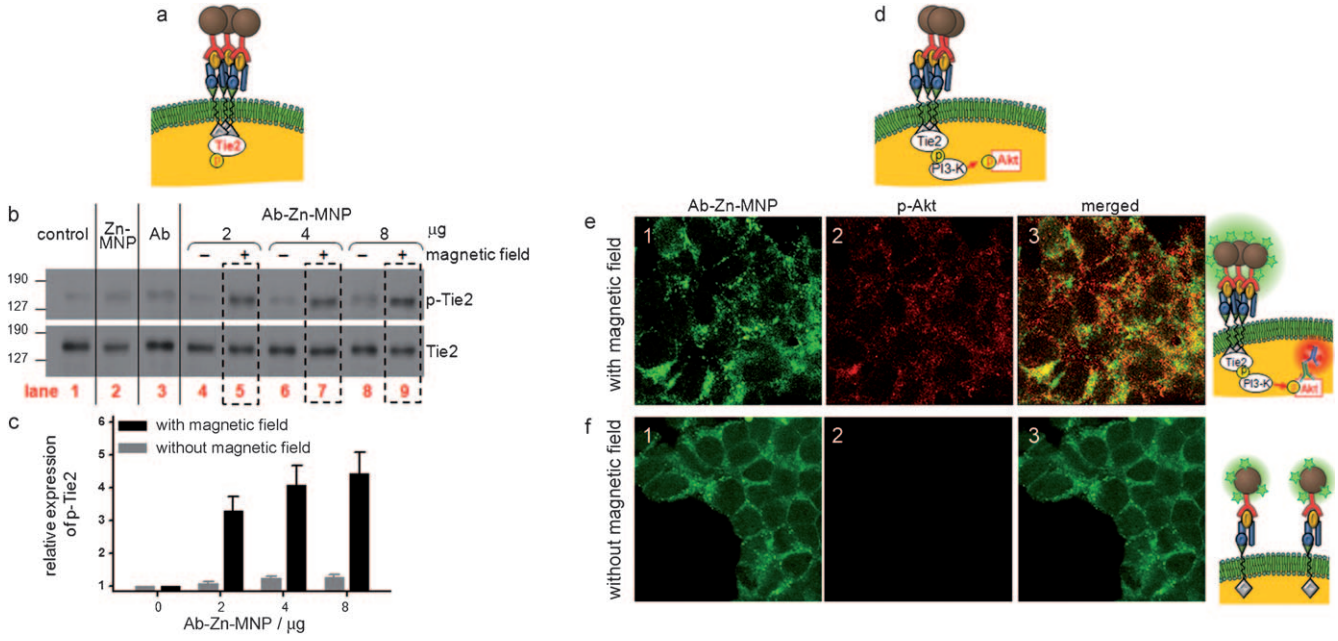

Figure 3. Intracellular signaling propagations induced by N-MACS. a) Phosphorylation of Tie2 (p-Tie2). b) Western blot analysis of 293-hTie2 cells which are stained with antibodies specific for p-Tie2 and Tie2; lane 1: control (293-hTie2 cell only), lane 2: bare Zn-MNP treated, lane 3: antibody-only treated, lanes 4–9: Ab-Zn-MNP treated without a magnetic field (−) or with a magnetic field (+). c) Relative expression of p-Tie2 versus the amount of Ab-Zn-MNP with or without application of an external magnetic field (three measurements; error bar: standard deviation). d) Phosphorylation of Akt (p-Akt). Fluorescence confocal microscopy images of cell cytoplasm after application of a magnetic field (e) and in the absence of a magnetic field (f), in which 1) Ab-Zn-MNP is labeled with fluorescein and 2) p-Akt is immunostained with anti-p-Akt IgG and anti-rabbit IgG–Alexa 594.

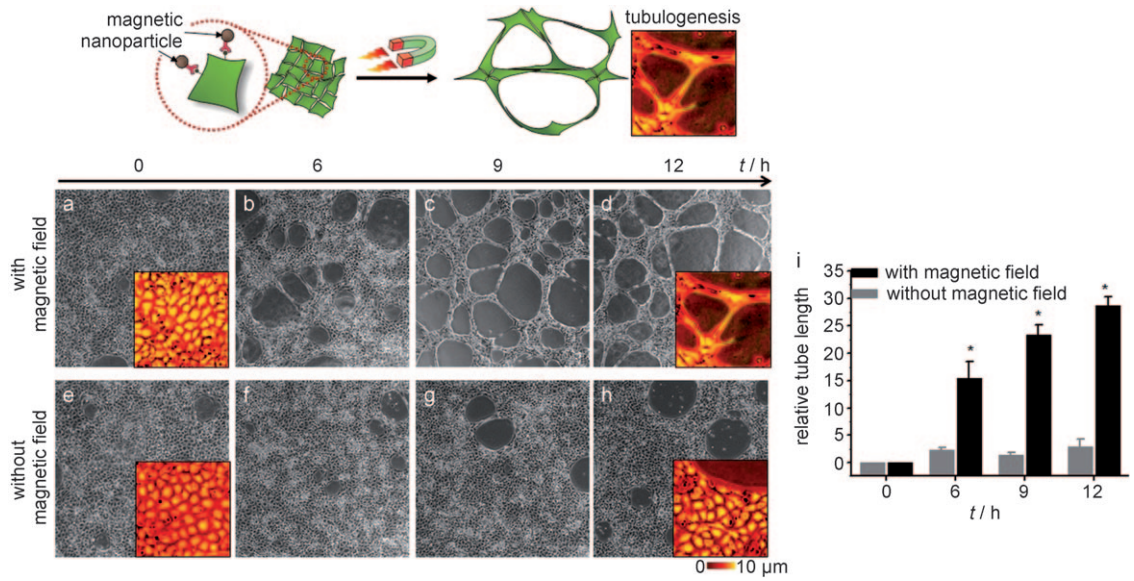

Figure 4. N-MACS on tubulogenesis of HUVECs at different time points after treatment with Ab-Zn-MNPs and application of a magnetic field (a–d) or without application of a magnetic field (e–h). Insets are magnified images of HUVECs, which are colored according to cell height from the bottom. i) Tube formation length of HUVECs with/without an external magnetic field (three measurements; error bar: standard deviation). Relative changes of tube length are shown in arbitrary units (*: $P < 0.0001$).

netic field is applied and that this process induces clustering of Tie2 receptors, which then triggers phosphorylation of Tie2 and further propagation of downstream signaling processes.

The study was extended to explore whether Tie2 receptor clusterization can initiate angiogenesis in the human umbilical vein endothelial cell (HUVEC), which is the main component comprising blood vessels that are known to possess a significant amount of Tie2 receptors.[23] The Ab-Zn-MNP (8 µg) was applied to HUVECs for 1 h at room temperature. After washing to remove unbound nanoparticles, a magnetic field of 0.15 T was applied in the same manner as in the 293-hTie2 cell experiments. The change of cellular morphology was examined by using differential interference contrast (DIC) microscopy for different times (0, 6, 9, and 12 h).

Initially, the cells have polygonal shapes and adhere to one another (Figure 4a,e, insets). When the cells are exposed to a magnetic field for 1 h, their shapes begin to progressively change to capillary-like tubular structures, which become abundant after 9 h of magnetic field application (Figure 4a–d). The shape transformation that takes place in HUVECs is commonly called tubulogenesis, which represents the preangiogenic stage eventually leading to blood vessel formation. In contrast, when a magnetic field is not applied, the shape change of the HUVECs is much slower (Figure 4e–h). This observation is quantified by measuring the length of tubes where the relative length to the initial cell size changes from 0 to 15.4, 23.3, and 28.7 as time increases (Figure 4i). These results clearly indicate that Tie2 signaling pathways in HUVECs are triggered by N-MACS and artificial angiogenesis is possible.

While some natural ligands such as angiopoietins can also induce similar effects, the N-MACS technique has unique advantages associated with the fact that it can be initiated remotely, noninvasively, and with temporal control. In addition, the methodology can be universally applied to various biological signaling processes.

Received: February 25, 2010
Published online: July 6, 2010

Keywords: angiogenesis · cellular signaling · magnetic properties · nanoparticles · receptors

[1] P. Fromherz, A. Offenhausser, T. Vetter, J. Weis, *Science* **1991**, *252*, 1290–1293.
[2] T. H. Young, C. R. Chen, *Biomaterials* **2006**, *27*, 3361–3367.
[3] J. Dai, M. P. Sheetz, *Biophys. J.* **1995**, *68*, 988–996.
[4] C. S. Chen, M. Mrksich, S. Huang, G. M. Whitesides, D. E. Ingber, *Biotechnol. Prog.* **1998**, *14*, 356–363.
[5] F. H. C. Crick, A. F. W. Hughes, *Exp. Cell Res.* **1950**, *1*, 37–80.
[6] P. A. Valberg, H. A. Feldman, *Biophys. J.* **1987**, *52*, 551–569.
[7] N. Wang, J. P. Butler, D. E. Ingber, *Science* **1993**, *260*, 1124–1177.
[8] M. Glogauer, J. Ferrier, C. A. McCulloch, *Am. J. Physiol. Cell Physiol.* **1995**, *269*, C1093–C1104.
[9] A. R. Bausch, W. Moller, E. Sackmann, *Biophys. J.* **1999**, *76*, 573–579.
[10] S. Na, O. Collin, F. Chowdhury, B. Tay, M. Ouyang, Y. Wang, N. Wang, *Proc. Natl. Acad. Sci. USA* **2008**, *105*, 6626–6631.
[11] R. J. Mannix, S. Kumar, F. Cassiola, M. Montoya-Zavala, E. Feinstein, M. Prentiss, D. E. Ingber, *Nat. Nanotechnol.* **2008**, *3*, 139–143.
[12] J. Dobson, *Nat. Nanotechnol.* **2008**, *3*, 139–143.
[13] S. Hughes, S. McBain, J. Dobson, A. J. El Haj, *J. R. Soc. Interface* **2008**, 5, 855–863
[14] L. Coultas, K. Chawengsaksophak, J. Rossant, *Nature* **2005**, *438*, 937–945.
[15] P. Carmeliet, *Nature* **2005**, *438*, 932–936.
[16] G. D. Yancopoulos, S. Davis, N. W. Gale, J. S. Rudge, S. J. Wiegand, J. Holash, *Nature* **2000**, *407*, 242–248.

[17] P. C. Maisonpierre, C. Suri, P. F. Jones, S. Bartunkova, S. J. Wiegand, C. Radziejewski, D. Compton, J. McClain, T. H. Aldrich, N. Papadopoulos, T. J. Daly, S. Davis, T. N. Sato, G. D. Yancopoulos, *Science* **1997**, *277*, 55 – 60.
[18] L. Eklund, B. R. Olsen, *Exp. Cell Res.* **2006**, *312*, 630 – 641.
[19] W. A. Barton, D. Tzvetkova-Robev, E. P. Miranda, M. V. Kolev, K. R. Rajashankar, J. P. Himanen, D. B. Nikolov, *Nat. Struct. Mol. Biol.* **2006**, *13*, 524 – 532.
[20] R. Harfouche, N. A. Malak, R. P. Brandes, A. Karsan, K. Irani, S. N. A. Hussain, *FASEB J.* **2005**, *19*, 1728 – 1730.
[21] J.-t. Jang, H. Nah, J.-H. Lee, S. H. Moon, M. G. Kim, J. Cheon, *Angew. Chem.* **2009**, *121*, 1260 – 1264; *Angew. Chem. Int. Ed.* **2009**, *48*, 1234 – 1238.
[22] R. R. White, S. Shan, C. P. Rusconi, G. Shetty, M. W. Dewhirst, C. D. Kontos, B. A. Sullenger, *Proc. Natl. Acad. Sci. USA* **2003**, *100*, 5028 – 5033.
[23] C. William, P. Koehne, J. S. Jürgensen, M. Gräfe, K. D. Wagner, S. Bachmann, U. Frei, K.-U. Eckardt, *Circ. Res.* **2000**, *87*, 370 – 377.

